Ferromagnetism in $Ga_{1-x}Mn_xP$: evidence for inter-Mn exchange mediated by localized holes within a detached impurity band

M. A. Scarpulla[1,2], B. L. Cardozo[1,2], R. Farshchi[1,2], W. M. Hlaing Oo[3], M. D. McCluskey[3], K. M. Yu[2], and O. D. Dubon[1,2, †]

[1]*Department of Materials Science & Engineering, University of California, Berkeley, CA 94720*

[2]*Lawrence Berkeley National Laboratory, Berkeley, CA 94720*

[3]*Department of Physics, Washington State University, Pullman, WA* 99164-2814

ABSTRACT

We report an energy gap for hole photoexcitation in ferromagnetic $Ga_{1-x}Mn_xP$ that is tunable by Mn concentration ($x \leq 0.06$) and by compensation with Te donors. For x~0.06, electrical transport is dominated by excitation across this gap above the Curie temperature (T_C) of 60 K and by thermally-activated hopping below T_C. Magnetization measurements reveal a moment of 3.9±0.4 μ_B per substitutional Mn while the large anomalous Hall signal unambiguously demonstrates that the ferromagnetism is carrier-mediated. In aggregate these data indicate that ferromagnetic exchange is mediated by holes localized in a Mn-derived band that is detached from the valence band.

PACS Numbers: 75.50.Pp, 72.60.+g, 75.47.-m, 73.50.Pz

† Corresponding author: oddubon@berkeley.edu

Diluted magnetic semiconductors (DMSs) are materials where a few atomic percent of a magnetic element is added to a non-magnetic semiconductor. Because of their unique combinations of magnetic and semiconducting properties and their potential for use as both injection sources and filters for spin-polarized carriers, these materials have been suggested for use in spin-based electronics, or spintronics. The discovery of ferromagnetism in $In_{1-x}Mn_xAs$ and $Ga_{1-x}Mn_xAs$ [1,2] ushered in more than a decade of intense experimental and theoretical research [3-6].

There is general consensus that the inter-Mn exchange in $Ga_{1-x}Mn_xAs$ and other ferromagnetic DMSs such as $Zn_{1-x}Mn_xTe$ [7] and $Ga_{1-x}Mn_xSb$ [8] is mediated by holes in extended or weakly localized states [9]. In GaAs, holes bound to Mn acceptors have a greater binding energy (~110 meV) and more localized wavefunctions than shallow acceptors [10]. The character of the mediating holes— valence band-like, impurity band-like, or mixed— is central to establishing accurate models for DMS ferromagnetism, yet this has not been conclusively established even for $Ga_{1-x}Mn_xAs$ [11,12]. With a larger hole binding energy for Mn acceptors (~400 meV) [13], Mn-doped GaP displays greater hole localization and is expected to have stronger p-d hybridization due to its shorter bond length. $Ga_{1-x}Mn_xP$ is thus an important test bed for understanding the interplay between localization and carrier-mediated exchange [14].

In this Letter, we present experimental evidence demonstrating carrier-mediated ferromagnetism in $Ga_{1-x}Mn_xP$ and the presence of a gap separating a Mn-derived band from the valence band. At low temperatures (i.e. $T<T_C$) holes are highly localized, but despite their strongly insulating nature $Ga_{1-x}Mn_xP$ films with nominal x~0.06 exhibit T_Cs

above 60 K. Previous reports [15] described unusual ferromagnetism in polycrystalline GaP layers containing Mn; however its origin was not conclusively established.

Samples for this study were prepared by ion implantation followed by pulsed-laser melting (II-PLM), which we have used to synthesize $Ga_{1-x}Mn_xAs$ layers with T_C up to 137 K [16-19]. This value should be compared to 173 K, the maximum T_C reported for films grown by molecular beam epitaxy and subjected to extended low-temperature annealing [20]. Briefly, unintentionally-doped (n-type, 10^{16}-10^{17} /cm^3) GaP (001) wafers were implanted with 50 keV Mn^+ to a dose of $2x10^{16}$ /cm^2. Some samples were additionally implanted with a matched depth profile of Te donors to intentionally lower the hole concentration. Each implanted sample was irradiated in air with a single 0.3-0.4 J/cm^2 pulse (FWHM = 18 ns) from a KrF excimer laser (λ = 248 nm) homogenized to a spatial uniformity of ±5% by a crossed-cylindrical lens homogenizer. Etching in concentrated HCl for ~24 hrs removed a poorly-regrown surface layer [17]. Channeling $^4He^+$ Rutherford backscattering spectrometry (RBS) and particle induced X-ray emission (PIXE) were used to assess the crystalline quality, total Mn and Te doses, and substitutional fractions of Mn and Te [21]. Secondary ion mass spectrometry (SIMS) reveals a Mn depth profile reaching a peak of x=0.06 at ~20 nm and extending to ~100 nm at which the Mn concentration has decreased by two orders of magnitude. SQUID magnetometry was used to measure magnetization and transport measurements were carried out in the van der Pauw geometry.

The solid line in the main panel of Fig. 1 presents the temperature variation of magnetization for a $Ga_{0.94}Mn_{0.06}P$ sample irradiated at 0.4 J/cm^2 measured along a [100] in-plane direction in a field of 50 Oe (after saturation to 50 kOe) while the inset depicts

the corresponding 5 K hysteresis loop. At 5 K the out-of-plane direction is found to be the hardest magnetization direction. A linear dependence of magnetization on temperature up to its T_C of 60 K is observed, which can be understood in terms of a small carrier density and/or carrier localization [18,22]. Samples irradiated between 0.3-0.35 J/cm^2 show a maximum T_C of 65 K while $Ga_{0.97}Mn_{0.03}P$ and $Ga_{0.96}Mn_{0.04}P$ films display T_Cs up to 23 and 42 K, respectively [17,23]. At 5 K the magnetization of the $Ga_{0.94}Mn_{0.06}P$ film saturates by 50 kOe at a value corresponding to 3.9±0.4 μ_B per *substitutional* Mn and 2.8±0.3 μ_B per *total* Mn. This reflects the measured Mn substitutionality of 70±5% which indicates an effective composition $x_{eff} \approx 0.04$. Because of the rapid solidification from the liquid phase involved in II-PLM, no appreciable Mn is present as interstitials as determined by RBS/PIXE measurements; the remaining 30% of Mn atoms likely exist as small clusters [21]. The dashed magnetization curve is from a sample compensated with Te; we interpret the decreased magnetization and T_C as being due to the partial compensation of the Mn. The compensation ratio, defined as the ratio of active Te to Mn concentrations, may be as high as 0.5 in some regions of the film; however, a reliable, depth-resolved measurement is not available. The changes in T_C accompanying variations of the Mn concentration and hole concentration (via compensation) are evidence that the ferromagnetism in $Ga_{1-x}Mn_xP$ is due to a carrier-mediated phase.

The filled circles in Fig. 2 represent the sheet resistivity of a $Ga_{0.94}Mn_{0.06}P$ sample with T_C = 60 K as a function of inverse temperature. The sample is clearly insulating and its resistivity is well described by a model of two thermally-activated processes:

$$\rho(T)^{-1} = (C_1 \exp\{E_1/k_BT\})^{-1} + (C_2 \exp\{E_2/k_BT\})^{-1} \qquad (1)$$

The free parameters are the activation energies $E_{1,2}$ and the pre-exponential constants $C_{1,2}$. Fitting the data to this simple model gives the high- and low-temperature activation energies as ~31 and ~6 meV, respectively. In p-type semiconductors, thermally-activated resistivity in the high-temperature range of the extrinsic regime is typically associated with hole transitions between the valence band and bound-acceptor states. Based on this and the spectroscopic data discussed below, we assign the high-temperature ~31 meV activation energy to excitation across a gap between a Mn-derived impurity band and the valence band. The fact that the change in slope occurs near T_C is consistent with the formation of a continuous hopping transport path at a percolation transition of magnetic polarons [24]. The small (6 meV) low-temperature activation energy is also consistent with this notion; however, other explanations may be possible. The open circles represent the resistivity of the sample in an applied field of 70 kOe while the inset shows that the magnetoresistivity (MR=ρ(70 kOe)/ρ(0)-1) is negative, reaching its largest magnitude of -48 % near T_C (60 K). Figure 3 presents the Hall resistance of the same sample as a function of applied field. The slope of the 300 K data indicates a hole concentration in the 10^{17}–10^{18} /cm^3 range, the uncertainty being due to a varying Mn composition as a function of depth and the strong anomalous Hall component which has the same sign as in $Ga_{1-x}Mn_xAs$ films. The magnitude of the anomalous component increases nearly linearly with decreasing temperature below T_C, reflecting the out-of-plane magnetization which is also fairly linear. These magnetoresistive and anomalous Hall characteristics reflect the intimate relationship between transport and ferromagnetism; similar behavior is observed in other III-V ferromagnetic

semiconductors [3,7] as well as in manganites [25]. Additionally, we have measured preliminary X-Ray absorption (XAS) and magnetic circular dichroism (XMCD) spectra at the Mn $L_{3,2}$ edge at 25 K and found that both the XAS and XMCD spectra are nearly identical to those from $Ga_{1-x}Mn_xAs$. The large (40%) XMCD asymmetry indicates a high spin polarization at the Fermi level [26].

To investigate the hypothesis of a Mn impurity band separated by an energy gap from the valence band, we used Fourier-transform infrared (IR) absorption and far-IR photoconductive (PC) spectroscopies. In PC spectroscopy, excitation of localized holes into extended states results in a change in conductivity that may be detectable by lock-in techniques with orders of magnitude greater sensitivity than may be achieved with absorption measurements. The extrinsic PC spectrum from a p-type semiconductor displays a threshold at a photon energy corresponding to the photoexcitation of holes from the neutral acceptor ground state to the valence band; this photoexcitation edge provides a close determination (within ~10%) of the hole binding energy.

The solid line in Fig. 4a shows the far IR photoconductivity response from the $Ga_{0.94}Mn_{0.06}P$ sample at 4.2 K while the dashed line gives the incident photon spectrum. The gross features of the incident spectrum are reproduced in the sample PC spectrum with the exception of the region below ~26 meV. The incident spectrum has appreciable spectral weight in this region; so the delayed onset of the sample response is strong evidence of an energy gap across which carriers are optically excited. This gap energy is in reasonable agreement with the ~31 meV energy deduced from the resistivity data. Together these suggest that the Mn impurity band is separated from the valence band (as

depicted in Fig. 4d) and that both the PC and resistivity measurements are due to hole transitions from the impurity band to the valence band.

To further test our hypothesis of a Mn impurity band separated by a gap from the valence band, we measured the photoconductivity spectra of films with lower Mn concentrations (i.e., $x<0.06$) and $Ga_{0.94}Mn_{0.06}P$ films compensated with Te donors. Decreasing the Mn concentration shifts the onset of the PC response to higher energies as well as increasing the activation energy for the high-temperature region of resistivity. These behaviors are consistent with narrowing of the impurity bandwidth with lower Mn concentration. In Te-compensated samples the onset of the PC response at 4.2 K occurs at ~70 meV (Fig. 4b), which is consistent with a shift of the Fermi energy (E_F) into the Mn band due to a reduction in hole concentration. The spectra in Fig. 4b taken at higher temperatures display a gradual increase in spectral weight at lower energies and a return of the PC onset to ~23 meV. Above 18.5 K the low-energy spectral weight continues to increase but the PC onset does not shift lower than 23 meV. We believe this behavior arises from the thermal redistribution of holes whereby the highest available impurity band (hole) states are occupied sufficiently at 18.5 K for detection via PC. Additionally, the resistivity of the Te-compensated sample displays an activation energy in the high-temperature region larger than that for $Ga_{0.94}Mn_{0.06}P$, reflecting a shift of E_F into the impurity band in agreement with the PC spectra. We note that no such temperature dependence of PC was observed in a sample containing only Mn ($x=0.04$) and having a 4.2 K PC onset of ~63 meV indicating negligible compensation in films doped only with Mn.

Figure 4c presents the IR absorption spectrum in the 150-650 meV energy range from a Te-compensated sample at 10 K. The spectrum is very weak and shows a broad feature peaked between 300-400 meV, which is near the Mn acceptor binding energy in GaP of 400 meV; we therefore interpret this broad feature as resulting from hole transitions from the Mn impurity band to the valence band. These data have been normalized to the spectrum from a sample which was implanted with 60 keV Ar^+ and laser melted under identical conditions; such normalization is used to remove absorption features not directly related to the presence of Mn such as those due to the excitation of GaP phonon modes or those due to the sample processing. The sharp dips in the spectrum reflect non-idealities in the normalization; nevertheless, the data clearly indicate a decrease of the absorption toward the lower photon energies, consistent with the PC results indicating a photoexcitation gap.

Models of carrier statistics involving an impurity band centered near 400 meV (with various densities of states) separated by a ~25 meV gap from the GaP valence band yield 300 K free-hole concentrations in the range of 10^{18}–10^{19} /cm^3 and can describe the observed temperature dependence of the resistivity at high temperatures (above T_C). This modeling and the experimentally observed resistivity indicate that the valence-band hole concentration is 1-2 orders of magnitude lower at the T_C of 60 K than our 300 K estimate of ~10^{18} /cm^3; it is therefore unlikely that models requiring large concentrations of valence-band holes that are on the order of the Mn concentration of 10^{20}-10^{21}/cm^3 can adequately account for the observed ferromagnetism.

The fundamental issue of whether the inter-Mn exchange (and hence T_C) changes monotonically across the Ga-Mn-pnictide series [27-29] is still unresolved. The shorter

bond length of GaP should lead to greater p-d exchange between holes and Mn ions than in GaAs. However, this increased exchange energy could contribute to the already significant localization of hole states leading to less overlap of states on different Mn and overall weaker inter-Mn exchange [14]. The presence of a distinct Mn impurity band and the ability to vary the Fermi energy via intentional compensation in $Ga_{1-x}Mn_xP$ enables testing theories of ferromagnetism and spin-polarized transport including the prediction of a change in sign of the anomalous Hall coefficient as the Fermi level moves within an impurity band [30].

In summary, $Ga_{1-x}Mn_xP$ represents a novel DMS system where strongly localized carriers in a detached impurity band stabilize ferromagnetism. The unique electrical, magnetic, and optical properties displayed by this material make it a model system for investigating the rich interplay between bandstructure, carrier localization, and mechanisms of ferromagnetic exchange.

This work was supported by the Director, Office of Science, Office of Basic Energy Sciences, Division of Materials Sciences and Engineering, of the US Department of Energy under Contract No. DE-AC03-76SF00098. We thank H. Ohldag and E. Arenholz for XAS/XMCD measurements, Y. Suzuki and E.E. Haller for use of facilities, I.D. Sharp, R. Chopdekar, T.W. Olson, and L.A. Reichertz for experimental assistance, and W. Walukiewicz for discussions.

REFERENCES

1. H. Ohno et al., Appl. Phys. Lett. **69** (3) 363 (1996).
2. H. Munekata et al., Phys. Rev. Lett. **63** (17) 1849 (1989).
3. H. Ohno, Science **281** 951 (1998).
4. T. Dietl, Semicond. Sci. Technol. **17** 377 (2002).
5. T. Dietl and H. Ohno, MRS Bul. **28** (10) 714 (2003).
6. F. Matsukura, H. Ohno, and T. Dietl, *Handbook of Magnetic Materials*, Vol. 14, ed. K. H. J. Buschow (Elsevier, Amsterdam, 2002), p. 1.
7. T. Dietl et al., in *Proceedings of the NATO Advanced Research Workshop "Recent Trends in Theory of Physical Phenomena in High Magnetic Fields*", eds. I. Vagner, et al. (Kluwer, Dordrecht, 2003), p. 197.
8. E. Abe et. al., Physica E **7** 981 (2000).
9. T. Dietl et al., Science **287** 1019 (2000).
10. M. Linnarsson et al., Phys. Rev. B **55**, 6938 (1997).
11. V.F. Sapega et al., Phys. Rev. Lett. **94**, 137401 (2005)
12. K.S. Burch et al., Phys. Rev. B **70** 205208 (2004) and references therein.
13. B. Clerjaud, J. Phys. C: Solid State Phys. **18** 3615 (1985) and references therein.
14. A.H. MacDonald, P. Schiffer, and N. Samarth, Nature Mater. **4** 195 (2005).
15. N. Theodoropoulou et al., Phys. Rev. Lett. **89** (10) 107203 (2002).
16. M. A. Scarpulla et al., Appl. Phys. Lett. **82** 1251 (2003).

17. M. A. Scarpulla et al., Physica B **340-342**, 908 (2003).

18. M. A. Scarpulla et al., in *Proceedings of the 27th International Conference on the Physics of Semiconductors*, eds. J. Menendez and C.G. Van de Walle, in press.

19. M. A. Scarpulla et al., in preparation.

20. K.Y. Wang et al., in *Proceedings of the 27th International Conference on the Physics of Semiconductors*, eds. J. Menendez and C.G. Van de Walle, in press.

21. K.M. Yu et al., Appl. Phys. Lett. **86** (4) 042102 (2005).

22. S. Das Sarma, E. H. Hwang, and A. Kaminski, Phys. Rev. B **67**, 155201 (2003).

23. O.D. Dubon et al., Phyisca B, *accepted* (2005).

24. A. Kaminski and S. Das Sarma, Phys. Rev. B. **68** 235210 (2003).

25. M. Viret, L. Ranno, and J.M.D. Coey, Phys. Rev. B **55** (13) 8067 (1997).

26. K.W. Edmonds, et al., Appl. Phys. Lett. **84** 4065 (2004).

27. P. Mahadevan and A. Zunger, Appl. Phys. Lett. **85** (14) 2860 (2004).

28. K. Sato et al., J. Magn. Magn. Mater. **272-276** 1983 (2004).

29. T. Jungwirth et al., Phys. Rev. B **66** (1) 012402 (2002).

30. A.A. Burkov and L. Balents, Phys. Rev. Lett. **91** (5) 057202 (2003).

FIGURE CAPTIONS

Figure 1 – (main) [100] in-plane magnetization measured as a function of temperature in $Ga_{0.94}Mn_{0.06}P$ (solid) and a $Ga_{0.94}Mn_{0.06}P$ sample compensated with Te (dashed). (inset) [100] in-plane magnetization of $Ga_{0.94}Mn_{0.06}P$ measured at 5 K.

Figure 2 – (main) Sheet resistivity (R_{sheet}) versus inverse temperature in zero-field for $Ga_{0.94}Mn_{0.06}P$ (filled circles) and Te-compensated $Ga_{0.94}Mn_{0.06}P$ (filled diamonds) as well as for $Ga_{0.94}Mn_{0.06}P$ at 70 kOe (open circles). The black line through the zero-field $Ga_{0.94}Mn_{0.06}P$ data is the fit to the model described in the text. (inset) Magnetoresistance between 70 and 0 kOe for $Ga_{0.94}Mn_{0.06}P$ as a function of temperature.

Figure 3 – Hall resistance as a function of magnetic field for $Ga_{0.94}Mn_{0.06}P$ showing the dominance of the anomalous component at low temperatures.

Figure 4 – (a) Far IR photoconductive response from $Ga_{0.94}Mn_{0.06}P$ sample (solid) and incident spectrum (dashed). An energy gap for photoexcitation is evidenced by the onset of the sample response at ~26 meV. (b) Far-IR PC response from a Te-compensated $Ga_{0.94}Mn_{0.06}P$ sample showing a larger gap (~70 meV) at 4.2 K, which decreases with increasing temperature. (c) Far-IR absorption spectrum from a Te-compensated sample at 10 K. The peak centered near 400 meV is due to the Mn impurity band. (d) Schematic density of states showing an energy gap separating the Mn impurity band from the valence band. The solid and dashed vertical lines in the impurity band indicate E_F at 0 K for $Ga_{1-x}Mn_xP$ ($x<0.06$) and Te-compensated samples, respectively, while the

corresponding arrows indicate the hole transitions responsible for the PC onset in each case. In the Te-compensated case, the PC onset shifts to lower energy for T>0 as states closer to the impurity band edge are thermally populated.

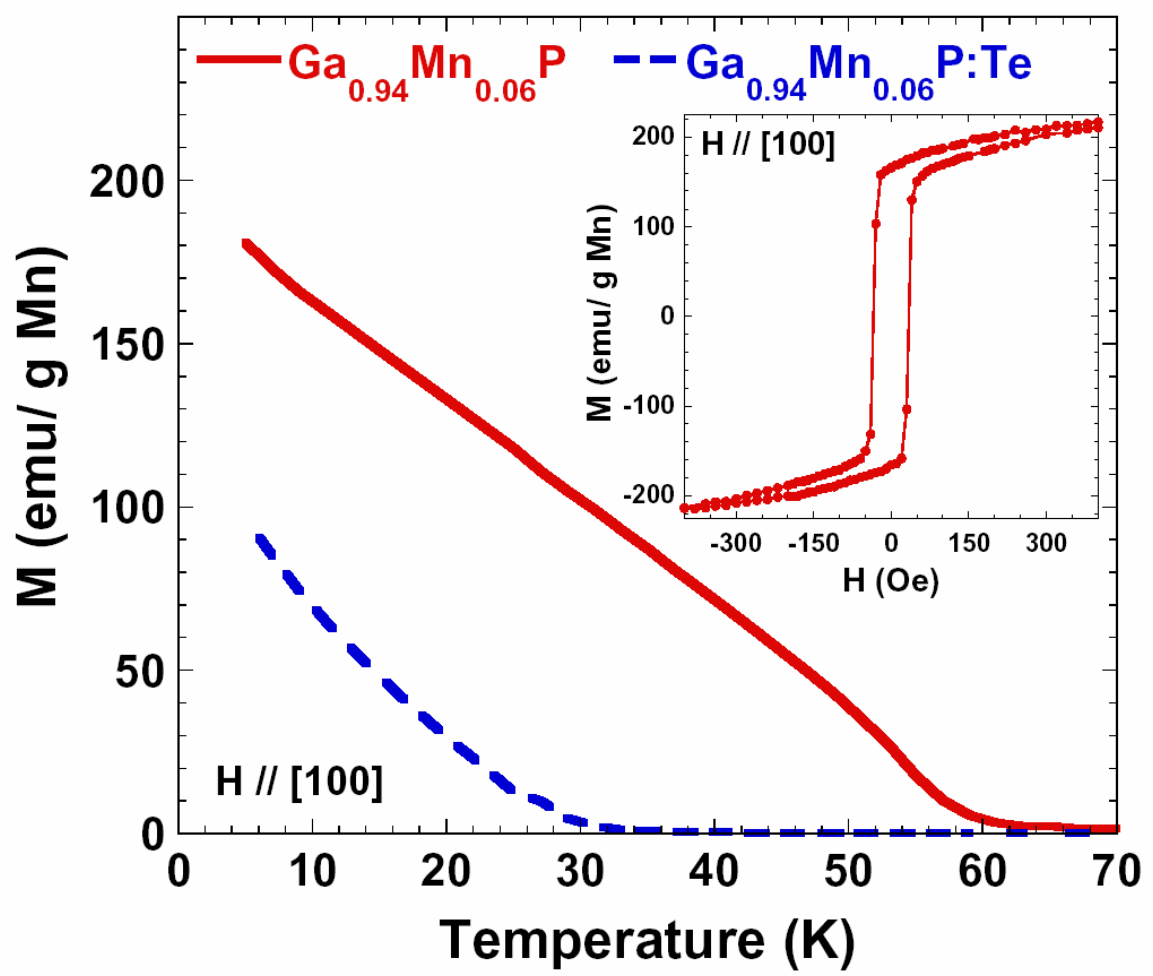
Ga0.94Mn0.06P
Ga0.94Mn0.06P:Te
H // [100]
M (emu/ g Mn)
Temperature (K)
0
50
100
150
200
0
10
20
30
40
50
60
70
H // [100]
M (emu/ g Mn)
H (Oe)
200
100
0
-100
-200
-300
-150
0
150
300

FIGURE 1

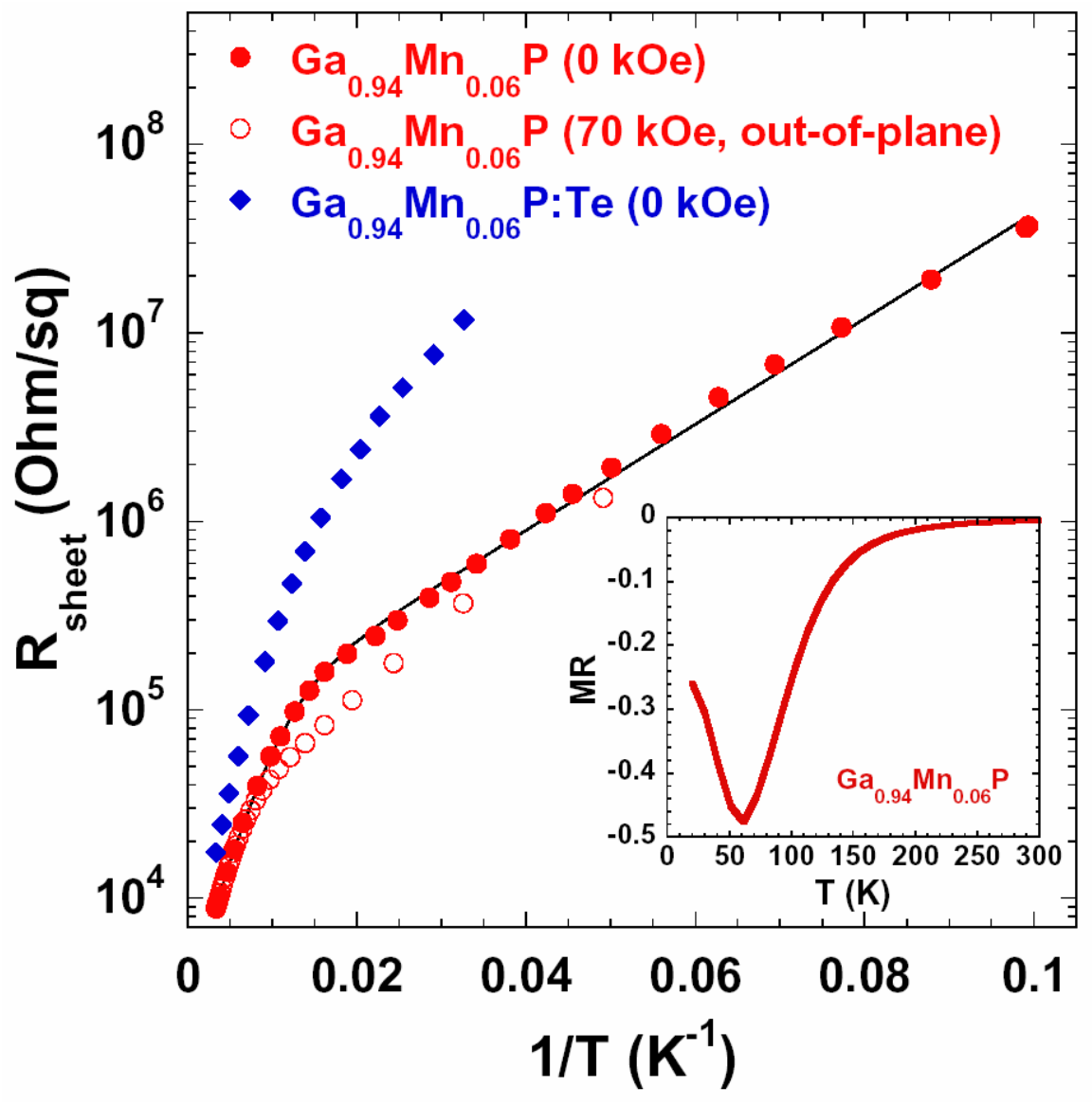
Ga0.94Mn0.06P (0 kOe)
Ga0.94Mn0.06P (70 kOe, out-of-plane)
Ga0.94Mn0.06P:Te (0 kOe)
R sheet (Ohm/sq)
10^8
10^7
10^6
10^5
10^4
0
0.02
0.04
0.06
0.08
0.1
1/T (K^-1)
MR
0
-0.1
-0.2
-0.3
-0.4
-0.5
0
50
100
150
200
250
300
T (K)
Ga0.94Mn0.06P

FIGURE 2

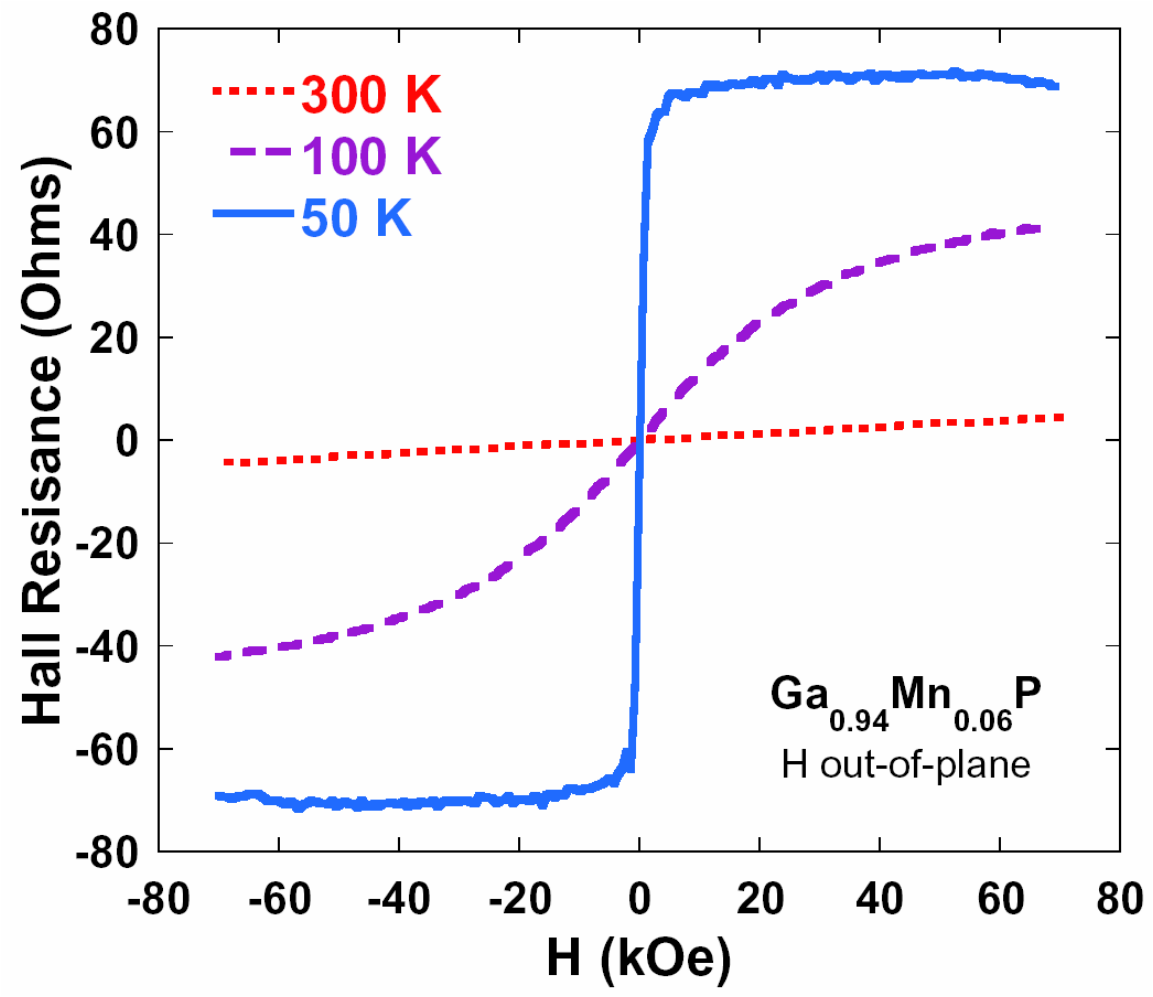
300 K
100 K
50 K
Hall Resisance (Ohms)
H (kOe)
Ga0.94Mn0.06P
H out-of-plane
80
60
40
20
0
-20
-40
-60
-80
-80
-60
-40
-20
0
20
40
60
80

FIGURE 3

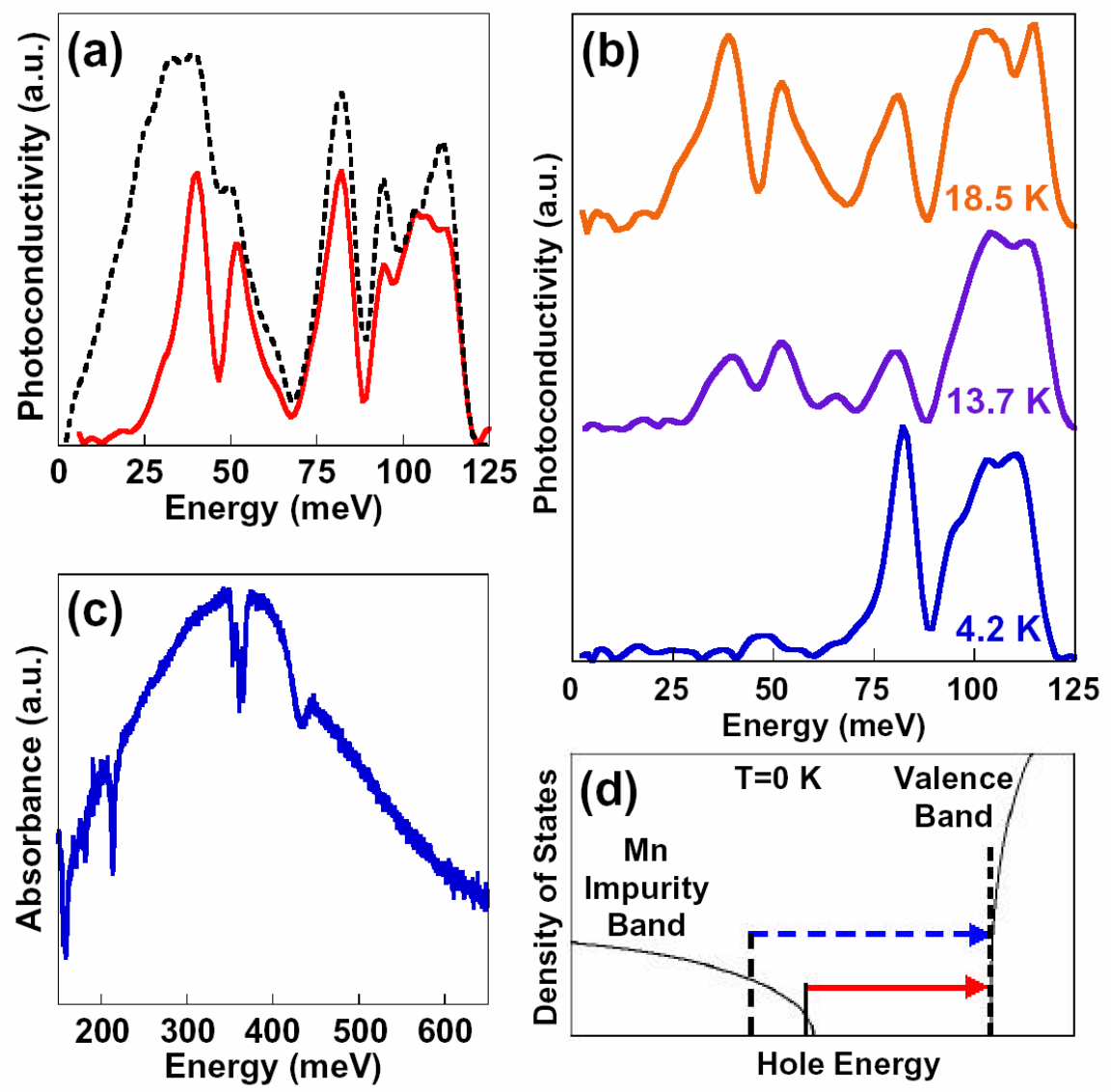
(a)
Photoconductivity (a.u.)
0
25
50
75
100
125
Energy (meV)
(b)
Photoconductivity (a.u.)
18.5 K
13.7 K
4.2 K
0
25
50
75
100
125
Energy (meV)
(c)
Absorbance (a.u.)
200
300
400
500
600
Energy (meV)
(d)
T=0 K
Valence Band
Mn Impurity Band
Density of States
Hole Energy

FIGURE 4